Journal of Biomolecular Structure and Dynamics

ISSN: (Print) (Online) Journal homepage: https://www.tandfonline.com/loi/tbsd20

Flavonoids as potential reactivators of structural mutation p53Y220C by computational and cell-based studies

Lakshay Malhotra, Punit Kaur & Abdul Samath Ethayathulla

To cite this article: Lakshay Malhotra, Punit Kaur & Abdul Samath Ethayathulla (2023): Flavonoids as potential reactivators of structural mutation p53Y220C by computational and cell-based studies, Journal of Biomolecular Structure and Dynamics, DOI: 10.1080/07391102.2023.2252071

To link to this article: https://doi.org/10.1080/07391102.2023.2252071

JOURNAL OF BIOMOLECULAR STRUCTURE AND DYNAMICS
https://doi.org/10.1080/07391102.2023.2252071

Flavonoids as potential reactivators of structural mutation p53Y220C by computational and cell-based studies

Lakshay Malhotra[a,b], Punit Kaur[a] and Abdul Samath Ethayathulla[a]

[a]Department of Biophysics, All India Institute of Medical Sciences, New Delhi, India; [b]Department of Biochemistry, Sri Venkateswara College, University of Delhi, New Delhi, India

Communicated by Ramaswamy H. Sarma

ABSTRACT

The p53 Y220C is one of the most frequently observed structural mutants in various human cancers. The substitution of residue Tyr to Cys makes the p53 DNA binding domain susceptible to solvent entry into the hydrophobic core of the domain thereby destabilizing p53, which results in loss of its tumor suppressor activity. The mutation creates a structural crevice at the region between S3/S4 and S7/S8 loops in the DNA binding domain which can be targeted by small molecules. Studies have shown that the synthetic and natural compounds could bind to this crevice and restore the structure and function of the mutant p53Y220C to the wild type. In our previous study, we have shown Curcumin could rescue the function of mutant p53Y220C in pancreatic cancer cell line BxPC-3 harboring genomic mutation. In this study, we explored six flavonoids structurally similar to Curcumin such as Apigenin, Isoliquiritigenin, Liquiritigenin, Luteolin, Methylophiopogonanone A (MPA), and Methylophiopogonanone B (MPB) to test their potency to restore p53Y220C by molecular docking, molecular dynamics simulations and cytotoxicity assay. The secondary structure analysis after the MD simulations suggested that these compounds could stabilize the mutant p53 DNA binding domain to the wild type. In the cell-based cytotoxicity studies using p53Y220C harbouring BxPC-3 cell lines, the compounds MPA and MPB showed 75% cell death at 100 μM concentration. We proposed that the flavonoids MPA and MPB have the therapeutic potential to restore p53Y220C and could be used as a combinatorial therapy to reduce the dosage burden.

ARTICLE HISTORY
Received 17 May 2023
Accepted 21 August 2023

KEYWORDS
p53Y220C; molecular docking; cytotoxicity; flavonoids; pancreatic cancer

1. Introduction

The p53Y220 is the seventh most frequently occurring mutation site of p53, comprising 143,000 cases/year. Among all p53Y220 mutations, just Y220C only accounts for 125,000 cases (which is ~1.8% of all p53 mutant tumors) and is reported in over 34 types of human tissues, (Bouaoun et al., 2016; Dumble et al., 2021; Malhotra et al., 2023; Olivier et al., 2010). According to the American Association of Cancer Research-Genomics, Evidence Neoplasia Information Exchange (AACR-GENIE) project cases, the maximum prevalence of this p53Y220C mutation is found in high-grade ovarian serous adenocarcinoma followed by pancreatic adenocarcinoma, breast invasive ductal carcinoma, lung adenocarcinoma, colon adenocarcinoma, etc. In the wild-type protein, the main role of Y220 is to guard the solvent entry inside the hydrophobic core of the protein. The presence of Cysteine at 220th residue fails to prevent the solvent entry and destabilizes the p53 DNA binding core domain leading to the loss of DNA binding ability (Bullock et al., 2000; Joerger et al., 2006; Joerger & Fersht, 2007; Malhotra et al., 2021). The inability of mutant p53Y220C to bind DNA seizes the tumor suppressor functions and transforms p53 into an oncogene resulting in tumorigenesis (Malhotra, 2023; Olivier et al., 2010).

Interestingly, this tyrosine-to-cysteine substitution creates a structural crevice or druggable pocket located far away from the DNA binding sites. To date, many small natural and synthetic molecules such as Curcumin, Withanolides, PC14586, PhiKan083, PK7088, PRIMA-1, etc have been targeted in this druggable site for structural and functional restoration of mutant p53Y220C (Bauer et al., 2019; Boeckler et al., 2008; Duffy et al., 2022; Izetti et al., 2014; Liu et al., 2013; Malhotra et al., 2022, 2021). Natural ligands are mostly considered safe and have more potent anti-cancerous effects when compared to synthetic ligands (Abu-Darwish & Efferth, 2018). Flavonoids are a class of natural compounds known to possess a wide range of anticancer properties by modulating reactive oxygen species (ROS), causing cell cycle arrest, inducing autophagy and apoptosis, and, suppressing tumor progression, etc (Batra & Sharma, 2013; Kopustinskiene et al., 2020; Tuli et al., 2023). These flavonoids are plant-based secondary metabolites that are commonly present in human foods and beverages and do not exhibit any side effects on the human body when compared to anti-cancerous drugs. The consumption of a flavonoid-rich diet endows the capability to combat cancers and also reduces the cancer risk by 20% (Havsteen, 2002; Veeramuthu et al., 2017). In our previous studies, we have shown that Curcumin, a flavonoid majorly found in *Curcumin longa*, not

CONTACT Abdul Samath Ethayathulla ethayathulla@aiims.edu Department of Biophysics, All India Institute of Medical Sciences, New Delhi 110029, India
Supplemental data for this article can be accessed online at https://doi.org/10.1080/07391102.2023.2252071.

only restores the secondary structure of the p53Y220C DNA binding domain (p53Y220C-DBD) but also rescues the transcription activity of this mutant p53 to the wild type (Malhotra et al., 2022, 2021). Curcumin specifically binds with mutant p53Y220C and restores the tumor suppressor activity to induce >80% cell death in pancreatic adenocarcinoma cells within 24 h (Malhotra et al., 2022). In this study, we have investigated the potency of some of the flavonoids such as Apigenin, Isoliquiritigenin, Liquiritigenin, Luteolin, Methylophiopogonanone A (MPA), Methylophiopogonanone B (MPB), which are structurally similar to Curcumin and possess no side effects on the human body. By employing the molecular docking studies, we have checked the binding affinity of these flavonoids in p53Y220C-DBD and also confirmed the stability of binding by molecular dynamics simulations and MM/PBSA free energy calculations. We have also established the impact of these molecules on the secondary structure content of p53Y220C. Finally, the potency of these natural compounds was substantiated in the BxPC-3 pancreatic adenocarcinoma cells harboring mutant p53Y220C.

2. Material and methods

2.1. Molecular docking

The molecular docking of flavonoids Apigenin, Isoliquiritigenin, Liquiritigenin, Luteolin, Methylophiopogonanone A, and Methyphiopoganone B was performed using AutoDock 4.2.6 with a similar protocol as described in our previous studies (Malhotra et al., 2021; Morris et al., 2009). The p53Y220C-DBD crystal [PDB ID:6SHZ_A] structure was used for docking the compounds after the removal of solvents and energy minimization. The crevice harboring the mutation Y220C was defined as the docking site as described in our previous studies. The coordinates of the flavonoids were obtained from PubMed and energy was minimized before docking. Out of 10 docked poses, the lowest free energy of binding conformation was selected as the best-docked state for each of the natural ligands. The selected docked conformations of various ligands and p53Y220C-DBD complex were further subjected to 100 ns molecular dynamics simulations to check the stability of bound compounds.

2.2. Molecular dynamics simulations

The molecular dynamics simulations were carried out using GROMACS-5.0.7 for all the screened natural ligands along with Curcumin as the positive control (Abraham et al., 2015; Berendsen et al., 1995). The best docked-ligand (flavonoid) topologies were generated using the PRODRG server without energy minimization (Schüttelkopf & van Aalten, 2004; van Aalten et al., 1996). The ".itp" and ".gro" ligand topologies obtained by the PRODRG server were then used along in complex with p53Y220C-DBD (topology generated by GROMACS) for MD simulations. The MD was performed with forcefield GROMOS 54a7 and the complex was placed in the cubic box of 10 Å from each direction of the protein atoms (Schmid et al., 2011). The ligand-protein complexes were solvated with the SPC216 water model and neutralized using three Cl^- atoms (Malhotra et al., 2021; Mark & Nilsson, 2001; Schmid et al., 2011). The solvated complex was energy minimized using the steepest descent algorithm with less than 1000.0 kJ/mol/nm convergent criteria with the subjection of 100 ns molecular dynamic simulation at a constant temperature of 300 K and pressure of 1 atm for 100 ps using the Berendsen thermostat Parrinello-Rahman barostat respectively, in the Periodic boundary condition. The Leapfrog Dynamics integrator was used for the integration of the position as well as the velocity of the atoms at the step size of 1 fs followed by the use of the LINCS algorithm for constraining all the bonds (Hess et al., 1997). PME (Particle Mesh Ewald) algorithm was used for the calculation of the long-range electrostatic forces whereas the cut-off scheme was used for calculating short-range forces *via* the Verlet scheme for the neighbor searching (Petersen, 1995). The same above protocol was used for the MD simulations of p53Y220C-DBD without ligands. The average H-bond occupancy, RMSD, RMSF, Radius of gyration (Rg), and Solvent accessible surface area were calculated for all protein-ligand complexes. The interactions between the ligands and p53Y220C-DBD at 0 and 100 ns were analyzed using Ligplot+ software (Wallace et al., 1995). The MM/PBSA free energy was calculated for all ligand-protein complexes *via* the g_mmpbsa module by GROMACS (using the default parameters) (Kollman et al., 2000; Kumari et al., 2014; Sharma et al., 2022; Srinivasan et al., 1998). The Sigmaplot 10.0 and XM Grace applications were used to create graphs and Pymol 2.4.1 was used for visualization and constructing structural figures (Seeliger & de Groot, 2010).

2.3. Secondary structure calculation

The secondary structure content was calculated for the p53Y220C-DBD in the presence and absence of all flavonoids after 100 ns MD simulations. The VMD_ss plugin (based on STRIDE) was used to calculate the secondary structure composition of the protein. The secondary structure contents of the flavonoid complexes were compared with the wtp53-DBD crystal structure (PDB ID: 3KMD)(Yahyavi et al., 2014).

2.4. ADMET analysis of flavonoids

For the calculations of physicochemical characteristics, solubility, drug-likeness properties, lipophilicity, and pharmacokinetic parameters, the SwissADME free-online server was used (Daina et al., 2017; Daina & Zoete, 2016). Also, the toxicological characteristics of all the flavonoids were predicted using the Osiris Data Warrior (Ajay Kumar et al., 2017).

2.5. Principal component analysis (PCA) and free energy landscape (FEL) analysis for MD simulations

The PCA was performed for the identification of the correlated motions of the p53wt/mutant-DBD (p53 wt and p53Y220C in the presence and absence of different ligands) derived from the conformational ensemble produced during the 100 ns of MD simulations (Sang et al., 2017; Tavernelli

et al., 2003). The gmx_covar gromacs utility was used for the generation of the C-alpha covariance matrix in the first step of PCA. The gmx_anaeig gromacs utility was used for the generation of the eigenvector followed by the generation of the Free energy landscape plot (Londhe et al., 2019; Motiwale et al., 2022; Wales & Bogdan, 2006).

2.6. Cell viability assay

To calculate the cytotoxicity of the flavonoids in the Human pancreatic BxPC-3 cancer cell lines, 8,000 cells per well were grown in a 96-well plate for 24 h in RPMI 1640 complete media (with 10% Fetal Bovine serum {South American Origin}, 1% Antibiotic and antimycotic from Gibco). The cells were then treated with different concentrations (0 to 100 μM for 24 h) of natural compounds like Apigenin, Isoliquiritigenin, Liquiritigenin, Luteolin, Methylophiopogonanone A, and Methyphiopoganone B with Curcumin as a positive control. The cell cytotoxicity of the ligand-treated and untreated cells was determined by 3-(4,5-Dimethylthiazol-2-yl)-2,5-Diphenyltetrazolium Bromide (MTT) using Molecular Probes, Invitrogen. The cells were incubated with MTT (0.5 mg/mL in PBS) at 37 °C under 5% CO_2 for 4 h. The existing solution containing media and MTT was then replaced with 80 μL of 100% DMSO followed by the measurement of absorbance for the dissolved blue formazone crystals at 575 nm using the Spectramax i3x (Malhotra et al., 2021). The cell viability assay was performed in 4 replicates and the graphs were made using Sigmaplot10.

3. Results

3.1. Molecular docking analysis

The docking study showed all six compounds (SMILES and PubChem ID are shown in Table S1) bind to the structural crevice of the DNA binding domain of p53Y220C (Figure 1). MPA and MPB showed the lowest binding energy of −10.08 kcal/mol while the remaining compounds ranged from −8 to −9 kcal/mol (Table 1).

The molecular docking showed that Apigenin forms three hydrogen-bonded interactions with backbone atoms of residues L145,T230 and T150 (Figure 1a). While Isoliquiritigenin and Liquiritigenin formed 6 and 3 hydrogen bonds, respectively, with backbone atoms of residues L145, V147, P152, G154, T155, and E221 (Figure 1b and c). The compound Luteolin formed six hydrogen-bonded interactions with backbone atoms of residues L145, V147, P152, and T155 (Figure 1d). In the case of MPA, four hydrogen-bonded interactions with L145, V147, G154, and T155 were observed. While MPB formed five hydrogen-bonded interactions with V147, T150, G154, and T155 (Figure 1f). Apart from hydrogen bonds, the hydrophobic interactions with the residues L145, V147, T150, P151, P152, P153, G154, P222, P223, and C220 were also observed with all compounds (Figure 1) (Tables 2 and S2). To further understand the stability of these compounds upon binding to the crevice, the flavonoid-p53Y220C-DBD complexes were subjected to 100 ns MD simulations studies.

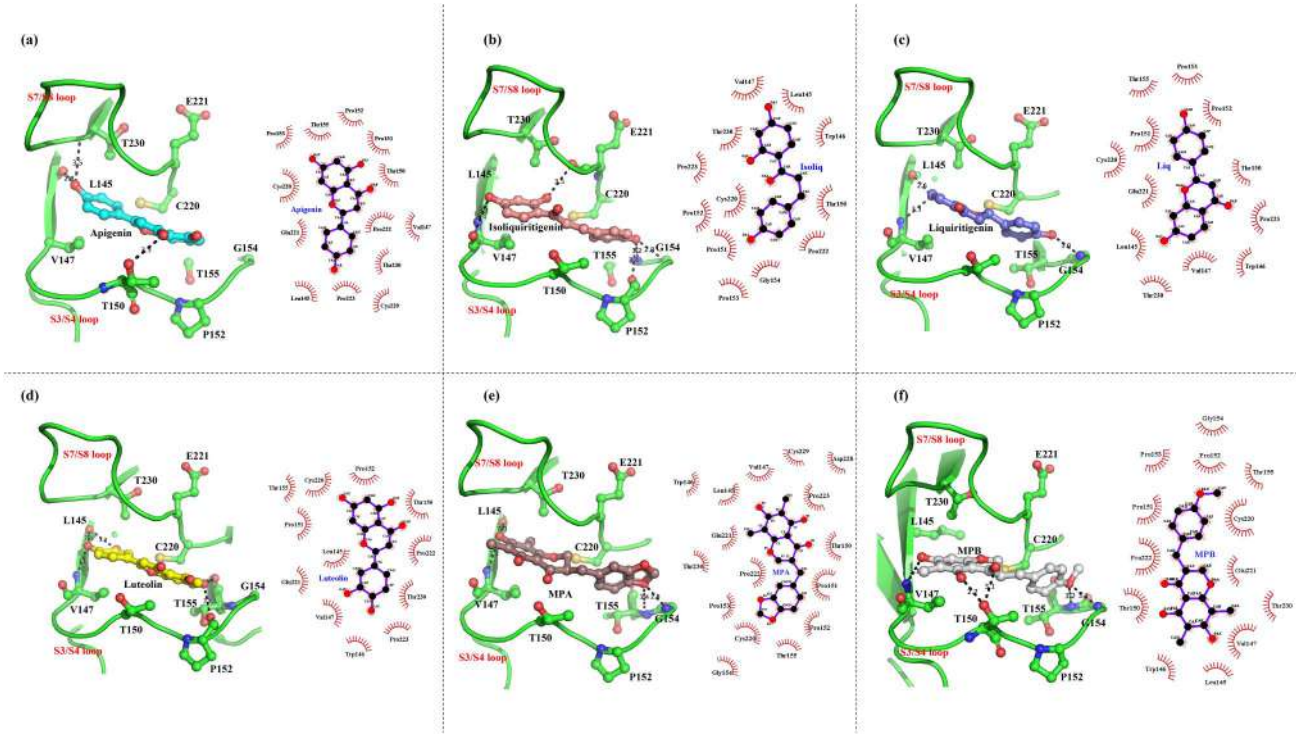

Figure 1. Docking of flavonoids in a p53Y220C-DBD structural crevice: the cartoon diagram shows the polar interactions and the ligplot represents the non-polar interaction formed between the p53Y220C-DBD and flavonoids (a) Apigenin, (b) Isoliquiritigenin, (c) Liquiritigenin, (d) luteolin, (e) MPA and (f) MPB. The residues forming the structural crevice are shown in ball and stick.

Table 1. Docked binding energy of flavonoids on p53Y220C-DBD.

S.No.	Ligand name	Structure	Binding energy (kcal/mol)
1.	**Apigenin**	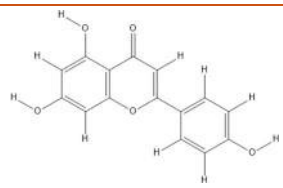	−8.40
2.	**Isoliquiritigenin**	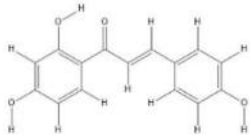	−8.55
3.	**Liquiritigenin**	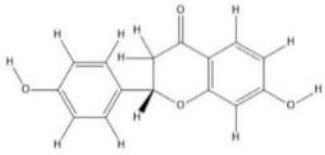	−8.85
4.	**Luteolin**	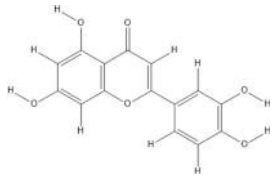	−8.36
5.	**MPB**	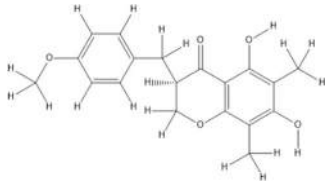	−10.08
6.	**MPA**	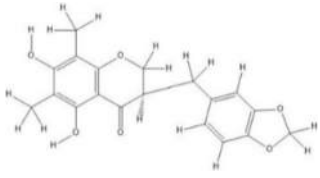	−10.08

3.2. Molecular dynamics simulations

The 100 ns MD simulations of all six flavonoid-p53Y220C-DBD complexes were carried out using gromacs. The overall RMSD calculations showed that all 6 complexes were stable throughout 100 ns of MD simulations (Figure 2a, Table S3). The radius of gyration of all the complexes was found to be constant throughout MD simulations. Upon analysis of the binding site of the mutant p53Y220C-DBD domain, no large conformational change was observed in the loops S3/S4 and S7/S8, and the shape of the structural crevice was maintained in the Apigenin and Luteolin complexes (Figure 2b, Table S3). While in other complexes, the compound binding induces a conformational change in the S7/S8 loop towards closed conformation thereby reducing the size of the cavity (Figure 2b, Table S3). Upon comparing the SASA (solvent accessible surface area) of protein in the presence and absence (nm^2) of ligand a slight decrease in SASA was observed (Table 3, Table S3).

Therefore, together indicating that the presence of these flavonoids at the druggable crevice could prevent solvent entry (Figure 2a) and stabilize the protein. All the flavonoids were intact inside the structural crevice throughout 100 ns of MD simulations (Figure 2b). The H-bond occupancy was also calculated for all six flavonoids.

After MD simulations Apigenin showed three stable hydrogen-bonded interactions throughout 100 ns with residues P152 and T155 (Figures 3a and S1a). While Isoliquiritigenin showed five constant H-bond with C220, P223, G226, D228, T230, and, Liquiritigenin formed 2 H-bonds with residues G226 and T230 (Figure 3b and 3c and Figure S1a). The compound Luteolin formed seven hydrogen-bonded interactions with L145, V147, P152, T155, and T230 (Figures 3d and S1a). In the case of MPA an average of 2 to 3 hydrogen-bonded interactions with backbone atoms of V147 (Figures 3e and S1a). While MPB forms an average of four hydrogen-bonded interactions with L145, V147, C229,

Table 2. Average number of H-bonds formed between the flavonoids and p53Y220C-DBD after molecular docking.

	Hydrogen bond distance (Å) and ligand atom					
Protein residues	Apigenin	Isoliquiritigenin	Liquiritigenin	Luteolin	MPA	MPB
L145 (O)	2.8 (OAR)	–	2.6 (OAS)	2.8 (OAS) 3.3 (OAR)	2.8 (O6)	–
V147 (NH)	–	3.1 (OAJ)	3.3 (OAS)	3.1 (OAS)	3.3 (O6)	3.1 (OAX)
V147 (O)	–	3.4 (OAJ)	–	–	-	–
T150 (OG1)	3.3 (OAB)	–	–	–	–	2.7 (OAW) 3.1 (OAB)
P152 (O)	–	3.4 (OAS)	–	3.1 (OAU)	–	–
G154 (NH)	–	2.8 (OAS)	3.0 (OAR)	–	2.8 (O4)	3.1 (OAU)
T155(NH)	–	3.2 (OAS)	–	–	3.4 (O4)	3.2 (OAU)
T155 (O)	–	–	–	3.0 (OAU)	–	–
E221 (O)	–	3.5 (OAI)	–	–	–	–
T230 (NH)	3.5 (OAR)	–	–	–	–	–

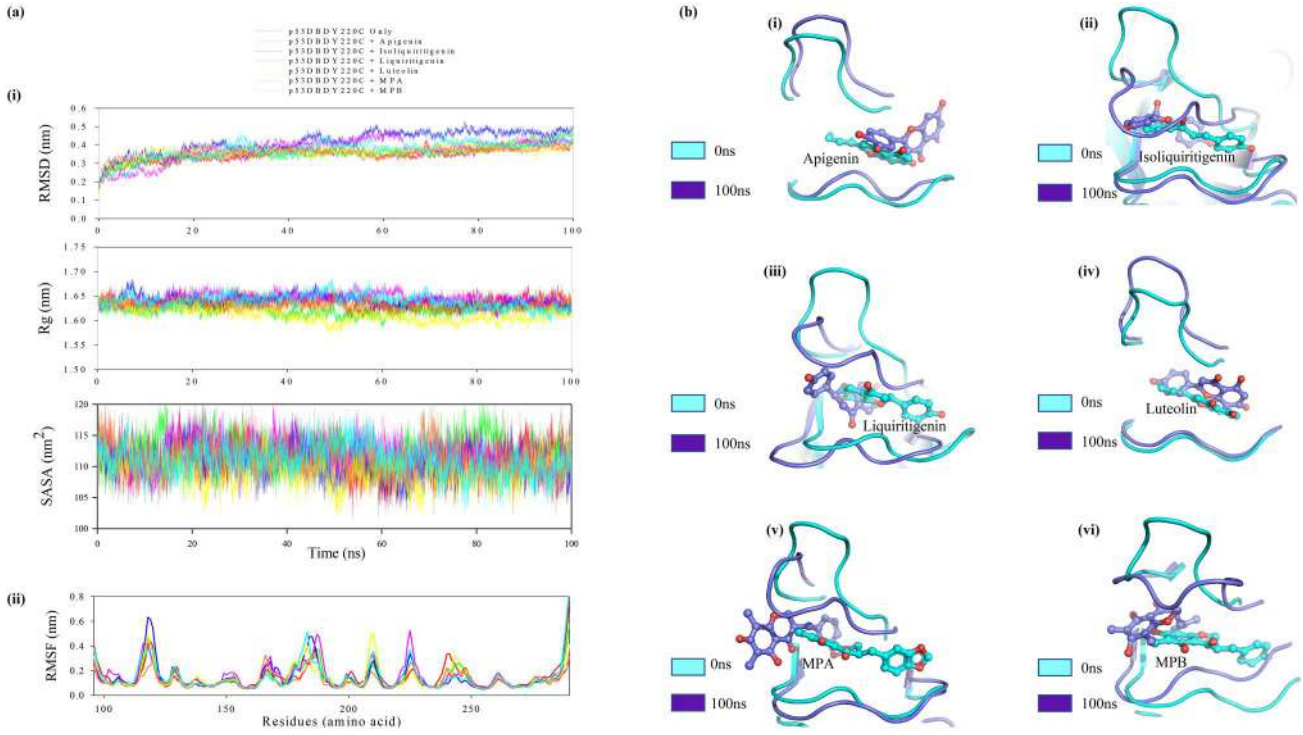

Figure 2. Molecular dynamics simulation of p53Y220C-DBD and flavonoids: (a) (i) the RMSD, Rg, SASA, and (ii) RMSF plots showing the stability of flavonoid-p53Y220C-DBD complexes in comparison to apo p53Y220C-DBD mutant. **(b)** Superimposition of the 0 and 100th frame of the MD simulations of all flavonoid complexes are shown in the cartoon (i) Apigenin, (ii) Isoliquiritigenin, (iii) Liquiritigenin, (iv) Luteolin, (v) MPA and (vi) MPB.

Table 3. The MD parameters of the p53Y220C-DBD in complex with and without ligands.

S.No.	Complexes	SASA nm^2	RMSD (nm) at 100 ns	Avg. RMSD (nm)	Rg (nm) at 100 ns	Avg. Rg (nm)	Avg RMSF (nm)
1	p53wt	108.922	0.324	0.308	1.628	1.637	0.125
2	p53Y220C only	113.439	0.402	0.348	1.631	1.637	0.151
3	Apigenin	109.113	0.442	0.356	1.610	1.623	0.138
4	Isoliquiritigenin	107.033	0.498	0.416	1.624	1.640	0.142
5	Liquiritigenin	108.046	0.428	0.373	1.638	1.645	0.156
6	Luteolin,	110.914	0.390	0.365	1.604	1.611	0.139
7	MPA	112.109	0.419	0.353	1.634	1.630	0.120
8	MPB	109.371	0.415	0.373	1.623	1.640	0.150

and T230 (Figures 3f and S1a). Apart from hydrogen bonds, all the compounds formed most of the hydrophobic interactions with the residues L145, V147, T150, P151, P152, P153, G154, P222, P223, C220, V225, S227, and C229 (Table 4). It is noted that both MPA and MPB formed Pi-Pi stacking interactions with W146 along with hydrogen-bonded interactions to keep them stable inside the structural crevice.

3.3. MM/PBSA calculations

The Gibbs free energy was calculated for all complexes. Among all six flavonoids, Isoliquiritigenin displayed the lowest free binding energy of −149.838 kJ/mol followed by MPB with the lowest binding energy of −126.754 kJ/mol. The compounds Liquiritigenin, Luteolin, MPA, and Apigenin showed interaction energy of −115.454, −101.823, −96.264,

and 90.713 kJ/mol, respectively. In comparison with Curcumin (-110.972 kJ/mol), the compound Isoliquiritigenin and MPB showed the lowest binding/interaction energy (Table 5). Figures S2a and S2b represent the total Apolar solvation energies and polar solvation energies of the whole flavonoid-ligand complexes throughout 100 ns of MD simulations. The Curcumin-p53Y220C-DBD was used as a control to understand the interaction energy of other flavonoid compounds. The MM/PBSA calculations show that the compounds are stable inside the structural crevice.

3.4. Secondary structure prediction

To understand the ligand-induced secondary structural change in the mutant p53Y220C-DBD, the STRIDE-based secondary

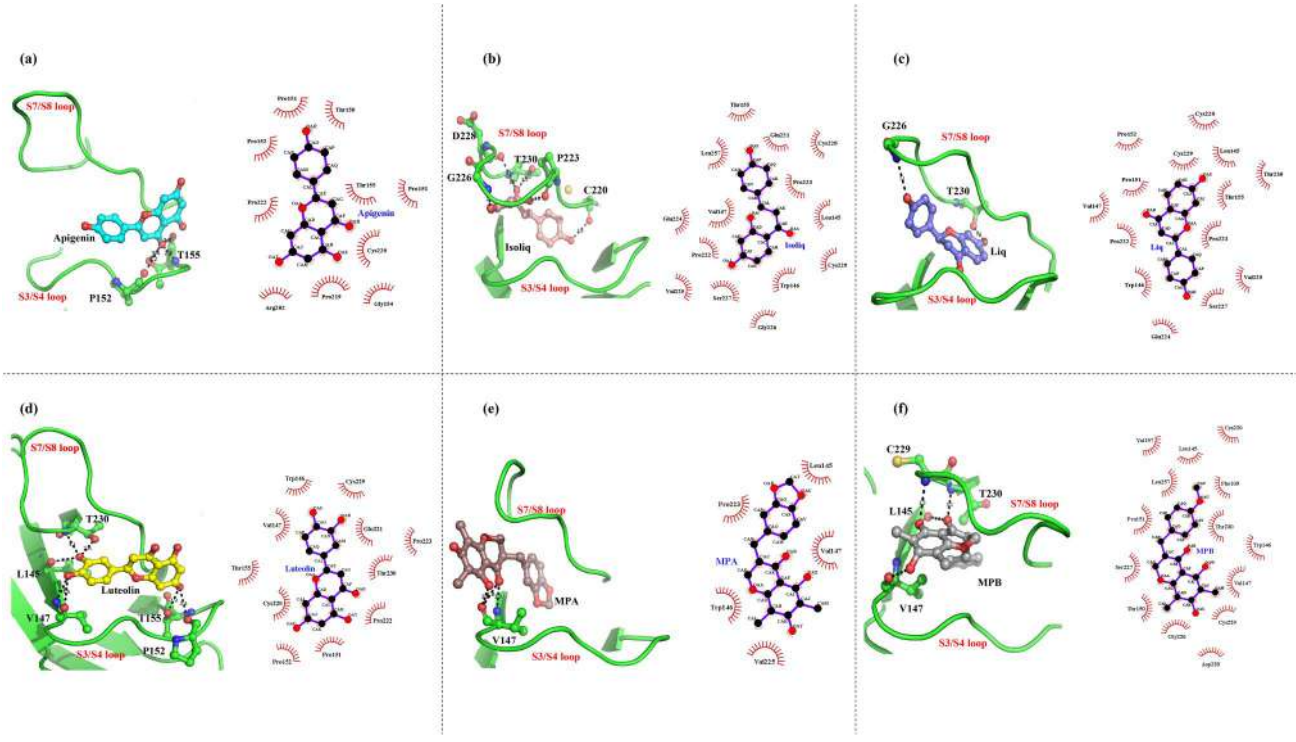

Figure 3. Polar and non-polar interactions of flavonoids-p53Y220C-DBD complex after MD simulations: the cartoon diagram shows the polar interactions formed between the p53Y220C-DBD and flavonoids after 100 ns of MD simulations (a) Apigenin, (b) Isoliquiritigenin, (c) Liquiritigenin, (d) Luteolin, (e) MPA and (f) MPB.

Table 4. List of hydrogen-bond and hydrophobic interactions formed by the p53Y220C-DBD residues with flavonoids after 100 ns of MD simulations.

	Hydrogen bond distance (Å) and ligand atom					
Protein residues	Apigenin	Isoliquiritigenin	Liquiritigenin	Luteolin	MPA	MPB
L145 (O)	–	–	–	3.1 (OAR)		3.3 (OAB)
L145 (N)	–	–	–	–		–
V147 (N)	–	–	–	2.9 (OAS)	2.6 (OAX)	–
V147 (O)	–	–	–	3.5 (OAS)	3.0 (OAB)	2.9 (OAX)
P152 (O)	3.2 (OAB)	–	–	3.4 (OAU)	–	–
T155 (NH)	2.6 (OAB)	–	–	–	–	–
T155 (OG1)	3.4 (OAB)			2.9 (OAU)	–	–
C220 (O)	–	2.9 (OAS)	–	–	–	–
P223 (O)	–	2.6 (OAI)	–	–	–	–
G226 (NH)	–	2.8 (OAJ)	3.3 (OAR)	–	–	–
D228 (O)	–	3.5 (OAA)	–	–	–	–
C229 (N)	–	–	–	–	–	3.3 (OAW)
T230 (N)	–	3.3 (OAA)	–	2.6 (OAR)	–	3.0 (OAB)
T230 (OG1)		3.5 (OAA)	2.6 (OAS)	3.1 (OAR)	–	–

Hydrophobic interactions

Ligand	**Protein residues**
Apigenin	T150, P151, P152, P153, G154, T155, R202, C220, P219, P222
Isoliquiritigenin	L145, W146, V147, T155, C220, E221, P222, P223, E224, V225, G226, S227, C229, L257
Liquiritigenin	L145, W146, V147, T155, C220, E221, P222, P223, E224, V225, G226, S227, C229, T230, L257
Luteolin	L145, W146, V147, P151, P152, T155, C220, E221, P222, P223, C229, T230
MPA	L145, W146, V147, C220, P222, P223, V225, S227, C229, L257
MPB	F109, L145, W146, V147, T150, P151, V157, C220, G226, S227, D228, C229, T230, L257

Table 5. MM/PBSA of the flavonoid-p53Y220C-DBD complex from 0-100 ns of MD simulations.

Energy (kJ/mol)	Apigenin	Isoliquiritigenin	Liquiritigenin	Luteolin	MPA	MPB	Curcumin
van der Waal energy	−123.158+/-14.77	−149.413+/-15.90	−150.638+/-22.03	−129.897 +/-15.26	−128.157 +/-16.02	−173.119 +/-18.30	−170.674 +/-15.66
Electrostatic energy	−27.558+/-11.13	−57.097+/-14.32	−27.928+/-15.33	−49.338+/-12.57	−16.310 +/-8.57	−25.397 +/-14.75	−41.489 +/-20.22
Polar solvation energy	72.318+/-14.97	72.318+/-14.97	77.406+/-17.11	90.893+/-10.38	61.297+/-19.96	88.336+/-20.66	119.409 +/-24.40
SASA energy	−12.315+/-1.30	−15.646+/-1.01	−14.294+/-1.49	−13.480+/-1.03	−13.093 +/-1.64	−16.574 +/-1.74	−18.218 +/-1.37
Binding energy	−90.713+/-16.19	−149.838+/-25.42	−115.454+/-19.09	−101.823 +/-11.88	−96.264 +/-22.00	−126.754 +/-19.57	−110.972 +/-16.10

structure calculation was carried out using the ss-VMD plugin. The wtp53-DBD (PDB ID: 3KMD) contains 9% α-Helix, 3% 3_{10} Helix, 35.02% β-sheet or extended configuration (E), 31.13% Turns (T), and 19.63% coil (Figure 4a) and after 100 ns MD simulations the mutant p53Y220C-DBD showed a significant reduction in the alpha-helical content (6.6%) compared to the wild type. In the case of flavonoid-p53Y220C-DBD complexes, except MPB all complexes showed a slight increase in the helical content of the mutant p53Y220C-DBD in the presence of Apigenin, Isoliquiritigenin, Liquiritigenin, Luteolin and MPA (Figure 4d–f, Table S4). For comparison, the secondary structure content of the p53Y220C-DBD-Curcumin complex was analyzed and it showed an increase in alpha helix, close to wild-type p53-DBD (Figure 4c). Both MM/PBSA and MD simulations studies establish that the flavonoids could bind to the structural crevice and stabilize the mutant p53 DNA binding domain. Hence, these compounds were further analyzed for the cytotoxicity assay.

3.5. ADMET analysis

From the ADMET (absorption, distribution, metabolism, excretion, and toxicity) analysis (conducted *via* SwissADME) it was found that Apigenin, MPA, and MPB are more bioavailable as these three compounds showed lipophilicity, polarity, properties of size, solubility, and saturation in the optimal range (Figure 5) (Figure S4-9). Further, the toxicity analysis of all these drugs was conducted using the Osiris Data Warrior software as shown in Table 6. It was found that both Apigenin and Isoliquiritigenin possess mutagenic properties when compared with other flavonoids. Also, Apigenin showed a mild risk of irritant properties. Therefore, among all six flavonoids Liquiritigenin, Luteolin, MPA, and MPB were found safer as a molecule. These drug-likeness properties as shown by the ADMET analysis in the bioavailability radar diagram along with the toxicity analysis by Osiris Data Warrior software signifies that both MPA and MPB are having upper hand in terms of drug-likeliness and as potential drug molecules when compared to other flavonoids. However, some scientific reports prove that Apigenin is non-mutagenic whereas Isoliquiritigenin possesses slightly weaker mutagenicity properties (Gulluce et al., 2013; Hashemi et al., 2010; Nagao et al., 1981; Wang et al., 2019).

The absorption of these flavonoids was also assessed and it was found that all these flavonoids have very high predicted GI absorption. Only Isoliquiritigenin, Liquiritigenin, and MPB showed the predicted property of crossing BBB (Blood-brain barrier) (Table 6, Figure S10).

3.6. Free energy landscape

The MD simulation-trajectory-based FEL analysis was conducted and it was found that the most stable poses of the wtp53-DBD exhibit the lowest free energy between 6 and 5.5 kcal/mol. On the other hand when the Y220C mutation is present in the protein then the most stable configurations/-poses were found at 10 kcal/mol basin (Figure 6). Interestingly in the presence of flavonoids such as Apigenin,

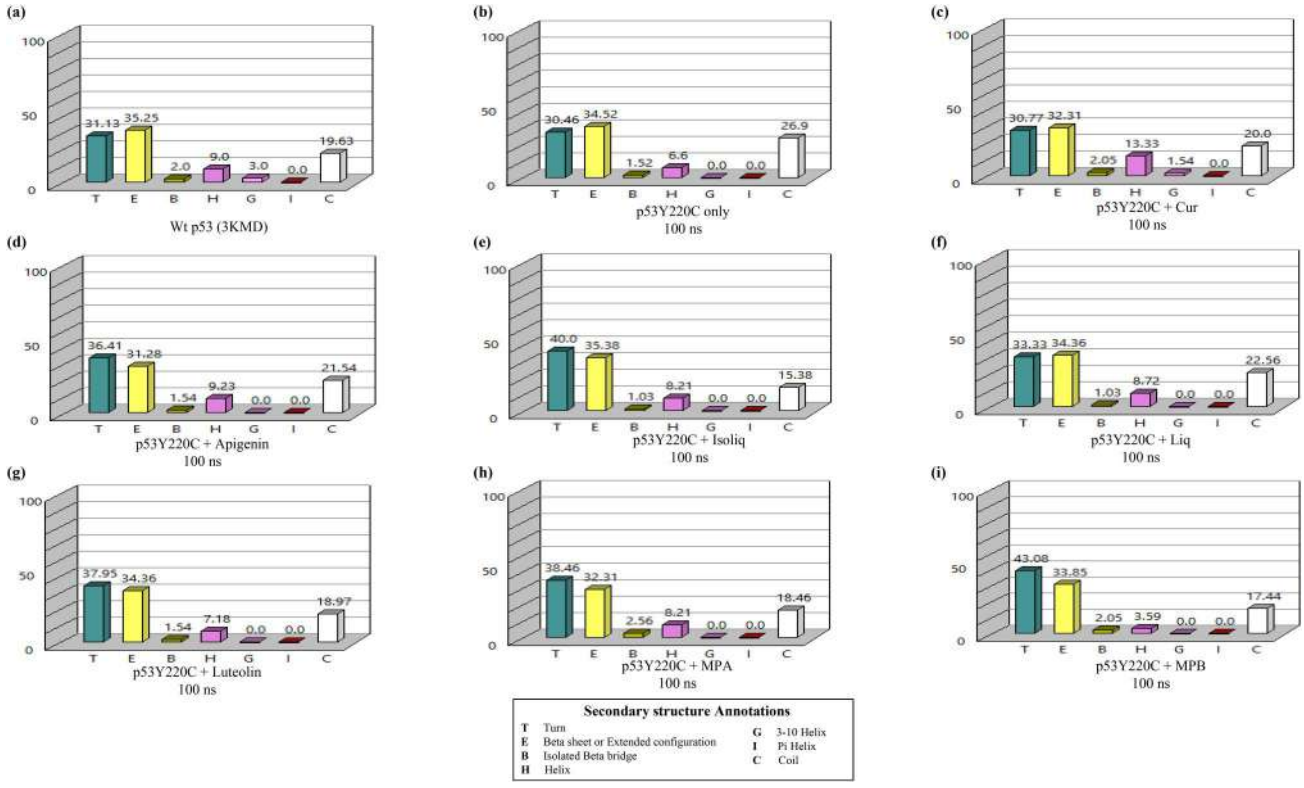

Figure 4. Secondary structure content analysis of flavonoid-p53Y220C-DBD complex after 100 ns MD simulation. The bar graphs represent the different structural components of (a) Crystal structure of wtp53-DBD (PDB ID: 3KMD), (b) p53Y220C-DBD without compound, (c) mutp53-DBD with Curcumin, (d) mutp53-DBD with Apigenin, (e) mutp53-DBD with Isoliquiritigenin, (f) mutp53-DBD with Liquiritigenin, (g) mutp53-DBD with luteolin, (h) mutp53-DBD with MPA, and (i) mutp53-DBD with MPB.

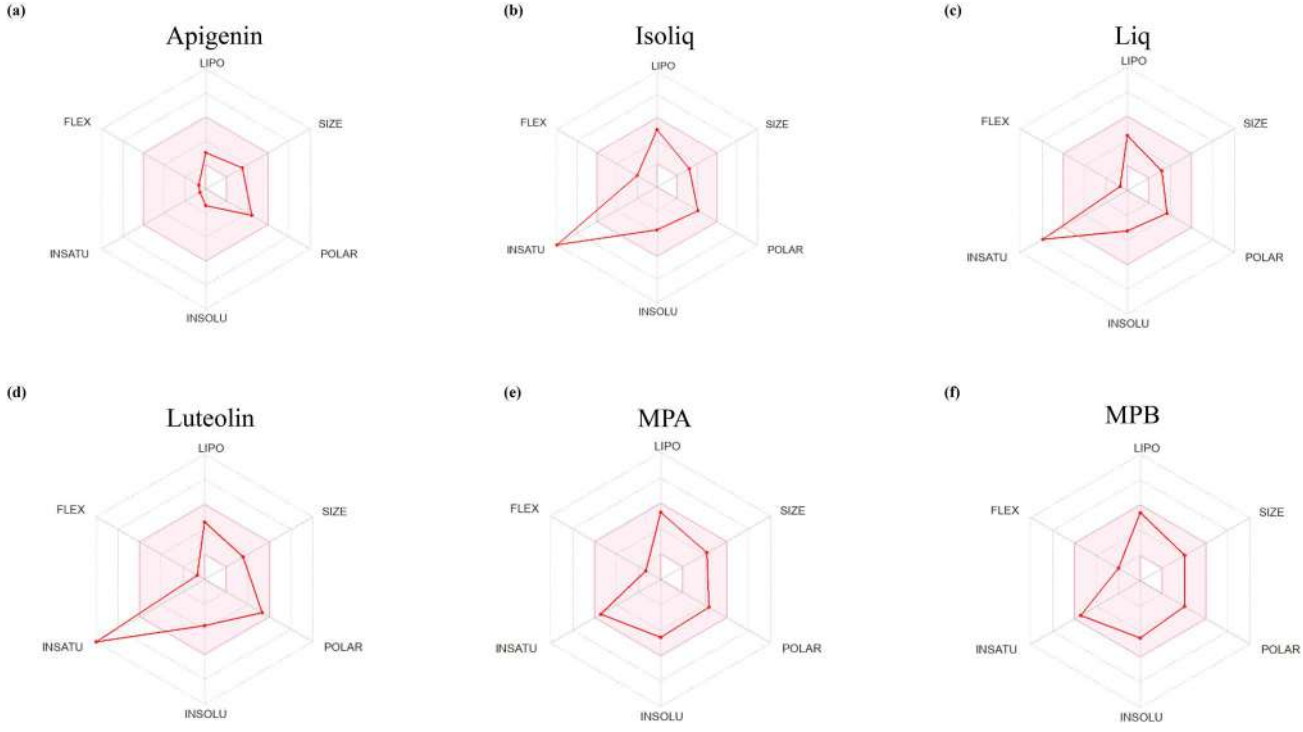

Figure 5. Bioavailability radar diagram of different natural flavonoids (a-f: Apigenin, Isoliquiritigenin, Liquiritigenin, Luteolin, MPA, MPB) showing different drug likeliness properties by SwissADME.

Luteolin, Liquiritigenin, MPA, and MPB the mutant protein got stabilized as the most stable poses showed the free energy lower than p53Y220C-DBD alone (Figure 6). This flavonoid-mediated p53Y220C-DBD stabilization was also validated by using Curcumin as a control. Curcumin presence successfully resulted in lowering the free energy of mutant protein as the lowest energy poses were found between 8 and 8.5 kcal/mol zone (Figure S11).

Table 6. Toxicity and absorption prediction of flavonoids by Osiris software and ADMET analysis.

S.No	Compound	Mutagenic	Tumorigenic	Irritant	Reproductive Effects	GI absorption	BBB permeant
1	Apigenin	High Risk	Low risk	Mild risk	Low risk	High	No
2	Isoliquiritigenin	High Risk	Low risk	Low risk	Low risk	High	Yes
3	Liquiritigenin	Low risk	Low risk	Low risk	Low risk	High	Yes
4	Luteolin	Low risk	Low risk	Low risk	Low risk	High	No
5	MPA	Low risk	Low risk	Low risk	Low risk	High	No
6	MPB	Low risk	Low risk	Low risk	Low risk	High	Yes

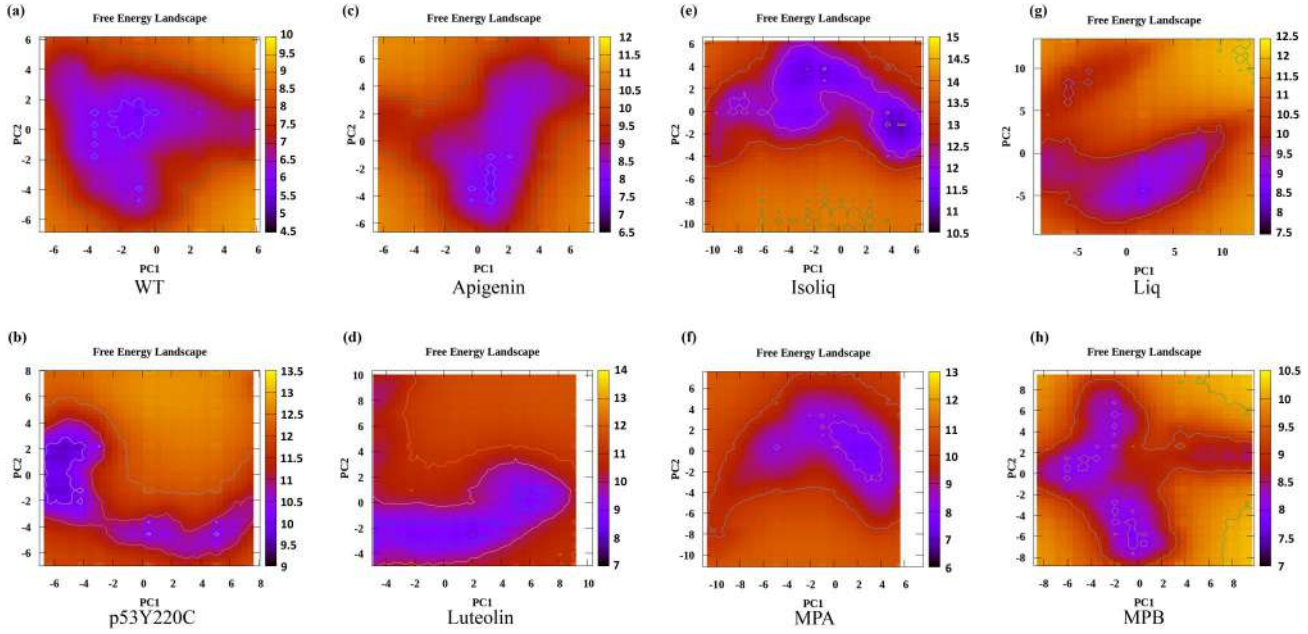

Figure 6. Free energy landscape of p53 wild type and Y220C mutant DBD in the absence and presence of flavonoids after 100 ns MD simulation. The FEL plots indicating the free energy on the right-axis (kcal/mol) for (a-b) p53 wild type and Y220C alone and in the presence of (c-h) Apigenin, Luteolin, Isoliquiritigenin, MPA, Liquiritigenin, and MPB.

On the other hand, the presence of Isoliquiritigenin was not able to put a significant impact on the mutant protein stability as the most stable poses were found between 10.5 and 11.5 kcal/mol basin (Figure 6).

3.7. Cell viability assay

For the cell cytotoxicity assay, Curcumin was used as control; as it has been established in our previously reported studies that at 3 μM concentration, 50% cytotoxicity was observed in the BxPC-3 pancreatic adenocarcinoma cells after 24 h of treatment. In comparison to Curcumin, only MPA and MPB showed 75% of cell death in BxPC-3 cell lines at 100 μM concentration. On the other hand, Isoliquiritigenin and Luteolin managed to kill 50% of the pancreatic cancer BxPC-3 cells at 100 μM concentration. The other two flavonoids Apigenin and Liquiritigenin showed $<$ 40% cell death in BxPC-3 cell lines (Figure 7, Figure S3, Table S5). It was found that all 6 flavonoids were able to cause cytotoxicity to a certain extent in the p53Y220C mutant cell lines but none of them were as efficient as Curcumin.

4. Discussion

Flavonoids are the polyphenolic plant secondary metabolites that are responsible for the color, flavor, and various pharmacological properties. Flavonoids are free radical scavengers, regulators of different cellular metabolism and possess anti-cancerous properties. Various reports showed that flavonoids execute the anti-cancerous properties by inhibiting the protein kinase B (Akt), phosphatidylinositide 3- kinase (PI3K), NF-κB, and epidermal growth factor receptor/mitogen-activated protein kinase (EGF/MAPK) pathways that lead to cell cycle arrest and apoptosis (Kopustinskiene et al., 2020). The p53Y220C structural and functional restoration is another strategy by which the natural flavonoid Curcumin mediates apoptosis (Malhotra et al., 2022, 2021). However, no other flavonoid is known to exhibit this p53 rescuer activity. In this study, we tried to explore the structural and functional restoration of p53Y220C by six different flavonoids using computational and cell-based studies.

Based on our molecular docking and MD results all 6 flavonoids can bind to the structural crevice formed by the S3/S4 and S7/S8 loop in mutant p53Y220C-DBD with binding energy in the range of −10 to −8 kcal/mol. Like Curcumin, all six flavonoids were found intact inside the structural crevice of the p53Y220C-DBD even after 100 ns of MD simulation indicating their stable binding. All these flavonoids showed reduced SASA at 100 ns compared to the native state of the mutant p53Y220C-DBD. Out of these six compounds, Isoliquiritigenin, Luteolin and MPB showed stable hydrogen-bonded interactions before and after MD simulations with lower binding energy calculated by MM/PBSA (Table 5). The

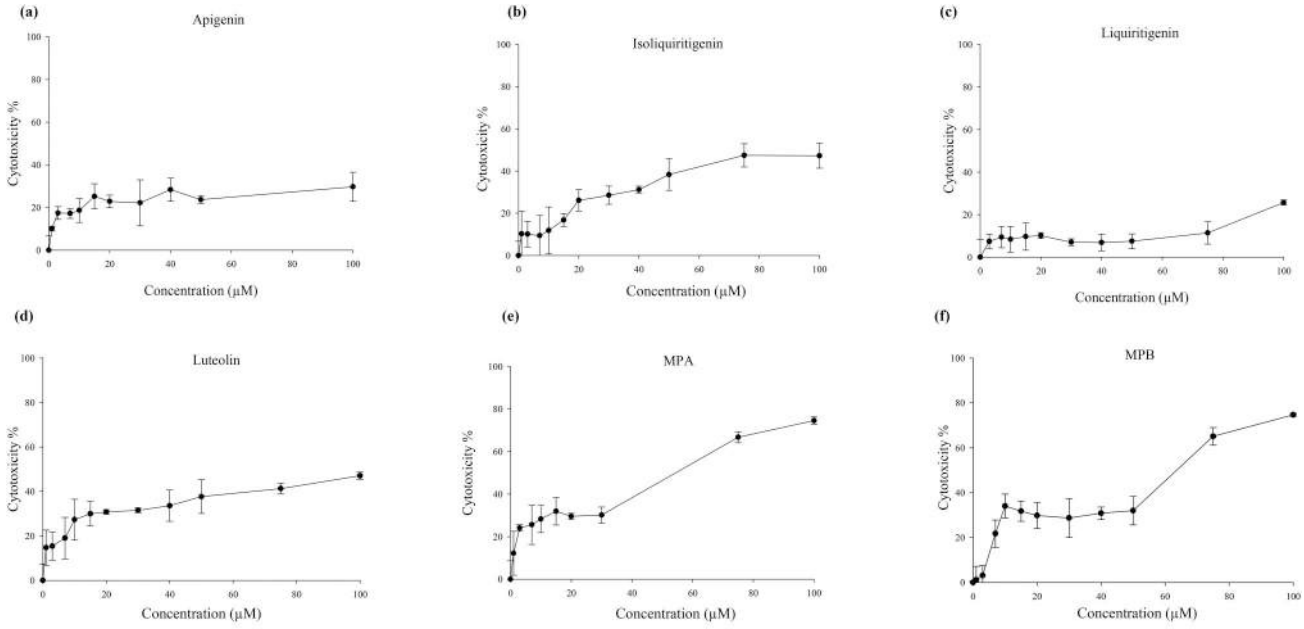

Concentration	Cytotoxicity (%) with SD					
	Apigenin	Isoliquiritigenin	Liquiritigenin	Luteolin	MPA	MPB
100 μM	29.74 +/- (6.807)	47.25 +/- (5.902)	25.70 +/- (1.171)	47.05 +/- (1.672)	74.55 +/- (1.705)	74.68 +/- (0.652)

Figure 7. Cell cytotoxicity assay of flavonoids in mutant BxPC-3 cells. The concentration-based cytotoxicity scatter-line graph representing the cytotoxicity in BxPC-3 cells after 24 h treatment of (a) Apigenin, (b) Isoliquiritigenin, (c) Liquiritigenin, (d) Luteolin, (e) MPA and (f) MPB.

compounds Luteolin and MPB are held by H-bond interactions with T230 at one end and with the backbone of L145 and V147 at another end of the crevice. In the case of Isoliquiritigenin, it is held by H-bond with T230 at one end and backbone interactions with C220, P223, and G226 at the end of the crevice. While in the case of MPA, at one end it is held by H-bond interactions with V147 and at the other end by hydrophobic interactions with less binding energy compared to MPB (Table 5). The FEL plot analysis of the MD simulation trajectories also showed that in the presence of the flavonoids the mutant protein poses lower free energy confirmations compared to p53Y220C alone, and the MD poses of the mutant Y220C are not as stable as the wild type (Figure 6). However, our cytotoxicity assay showed only MPA and MPB showed 75% cell death at 100 μM concentration while other compounds with 50% or less cytotoxicity.

In the literature, it has been reported that Apigenin at 100 μM showed 50% cytotoxicity in pancreatic adenocarcinoma BxPC-3 by transcription-independent p53 activity (King et al., 2012). However, the underlying mechanism of action of Apigenin-mediated mutant p53 was never explored in depth. Our results indicated that Apigenin might restore mutant p53Y220C fold and initiate its transcription-independent function. However, among all six flavonoids, MPA, MPB, and Isoliquiritigenin showed better cytotoxicity than Apigenin. In comparison to Curcumin, none of the flavonoids showed the greater cytotoxicity. The ADMET analysis also indicated that out of these 6 compounds, the compounds MPA and MPB are the best bioavailable molecules due to their physical properties and non-toxic nature. Although the compound Isoliquiritigenin have stable H-bonded interactions with good binding energy it possesses high mutagenic property (Figure 5) and hence may not be an ideal candidate compared to MPA and MPB.

Together, our all results indicated that the flavonoids MPA and MPB are the best flavonoids used in this study. However, all 6 flavonoids have the potential to restore the p53Y220C but need more structural modifications (especially MPA and MPB) to reduce the dosage burden of other p53Y220C drugs.

However, more structural modification and biochemical studies are required to make these natural flavonoids more potent anticancer molecules.

Ethical approval

The article does not involve any study with human participants or animals performed by any of the authors.

CRediT authorship contribution statement

LM: Methodology, Validation, Formal analysis, Investigation, Data curation, Graphics generation, Software, Writing, Review & editing, and Visualization. **PK:** review and editing **ASE:** Methodology, Validation, Formal analysis, Investigation, Data curation, Writing - Review & editing and Visualization.

Disclosure statement

No potential conflict of interest was reported by the authors.

Funding

This work was financially supported by grants from AIIMS (A-909), ICMR (5/13/72/2020/NCD-III), and DBT project DRF:51 (Department of Biotechnology, India).

ORCID

Lakshay Malhotra http://orcid.org/0000-0001-6700-5330
Abdul Samath Ethayathulla http://orcid.org/0000-0001-8958-3916

References

Abraham, M. J., Murtola, T., Schulz, R., Páll, S., Smith, J. C., Hess, B., & Lindahl, E. (2015). GROMACS: High performance molecular simulations through multi-level parallelism from laptops to supercomputers. *SoftwareX*, *1-2*, 19–25. https://doi.org/10.1016/j.softx.2015.06.001

Abu-Darwish, M. S., & Efferth, T. (2018). Medicinal plants from near east for cancer therapy. *Frontiers in Pharmacology*, *9*, 56. https://doi.org/10.3389/fphar.2018.00056

Ajay Kumar, T. V., Kabilan, S., & Parthasarathy, V. (2017). Screening and toxicity risk assessment of selected compounds to target cancer using QSAR and pharmacophore modelling. *International Journal of PharmTech Research*, *10*(4), 219–224. https://doi.org/10.20902/IJPTR.2017.10428

Batra, P., & Sharma, A. K. (2013). Anti-cancer potential of flavonoids: Recent trends and future perspectives. *3 Biotech*, *3*(6), 439–459. https://doi.org/10.1007/s13205-013-0117-5

Bauer, M. R., Jones, R. N., Tareque, R. K., Springett, B., Dingler, F. A., Verduci, L., Patel, K. J., Fersht, A. R., Joerger, A. C., & Spencer, J. (2019). A structure-guided molecular chaperone approach for restoring the transcriptional activity of the p53 cancer mutant Y220C. *Future Medicinal Chemistry*, *11*(19), 2491–2504. https://doi.org/10.4155/fmc-2019-0181

Berendsen, H. J. C., van der Spoel, D., & van Drunen, R. (1995). GROMACS: A message-passing parallel molecular dynamics implementation. *Computer Physics Communications*, *91*(1–3), 43–56. https://doi.org/10.1016/0010-4655(95)00042-E

Boeckler, F. M., Joerger, A. C., Jaggi, G., Rutherford, T. J., Veprintsev, D. B., & Fersht, A. R. (2008). Targeted rescue of a destabilized mutant of p53 by an in silico screened drug. *Proceedings of the National Academy of Sciences of the United States of America*, *105*(30), 10360–10365. https://doi.org/10.1073/pnas.0805326105

Bouaoun, L., Sonkin, D., Ardin, M., Hollstein, M., Byrnes, G., Zavadil, J., & Olivier, M. (2016). TP53 variations in human cancers: New lessons from the IARC TP53 database and genomics data. *Human Mutation*, *37*(9), 865–876. https://doi.org/10.1002/humu.23035

Bullock, A. N., Henckel, J., & Fersht, A. R. (2000). Quantitative analysis of residual folding and DNA binding in mutant p53 core domain: Definition of mutant states for rescue in cancer therapy. *Oncogene*, *19*(10), 1245–1256. https://doi.org/10.1038/sj.onc.1203434

Daina, A., Michielin, O., & Zoete, V. (2017). SwissADME: A free web tool to evaluate pharmacokinetics, drug-likeness and medicinal chemistry friendliness of small molecules. *Scientific Reports*, *7*(1), 42717. https://doi.org/10.1038/srep42717

Daina, A., & Zoete, V. (2016). A boiled-egg to predict gastrointestinal absorption and brain penetration of small molecules. *ChemMedChem*, *11*(11), 1117–1121. https://doi.org/10.1002/cmdc.201600182

Duffy, M. J., Tang, M., Rajaram, S., O'Grady, S., & Crown, J. (2022). Targeting mutant p53 for cancer treatment: Moving closer to clinical use? *Cancers*, *14*(18), 4499. https://doi.org/10.3390/cancers14184499

Dumble, M., Xu, L., Dominique, R., Liu, B., Yang, H., McBrayer, M.-K., Thomas, D., Fahr, B., Li, H., Huang, K.-S., Robell, K., Mulligan, C., Russo, B., Puzio-Kuter, A., Davis, T., & Vu, B. (2021). Abstract LB006: PC14586: The first orally bioavailable small molecule reactivator of Y220C mutant p53 in clinical development. *Cancer Research*, *81*(13_Supplement), LB006. https://doi.org/10.1158/1538-7445.AM2021-LB006

Gulluce, M., Orhan, F., Adiguzel, A., Bal, T., Guvenalp, Z., & Dermirezer, L. O. (2013). Determination of antimutagenic properties of apigenin-7-O-rutinoside, a flavonoid isolated from Mentha longifolia (L.) Huds. ssp. longifolia with yeast DEL assay. *Toxicology and Industrial Health*, *29*(6), 534–540. https://doi.org/10.1177/0748233712442732

Hashemi, M., Nouri Long, M., Entezari, M., Nafisi, S., & Nowroozii, H. (2010). Anti-mutagenic and pro-apoptotic effects of apigenin on human chronic lymphocytic leukemia cells. *Acta Medica Iranica*, *48*(5), 283–288.

Havsteen, B. H. (2002). The biochemistry and medical significance of the flavonoids. *Pharmacology & Therapeutics*, *96*(2–3), 67–202. https://doi.org/10.1016/S0163-7258(02)00298-X

Hess, B., Bekker, H., Berendsen, H. J. C., & Fraaije, J. G. E. M. (1997). LINCS: A linear constraint solver for molecular simulations. *Journal of Computational Chemistry*, *18*(12), 1463–1472. https://doi.org/10.1002/(SICI)1096-987X(199709)18:12<1463::AID-JCC4>3.0.CO;2-H

Izetti, P., Hautefeuille, A., Abujamra, A. L., de Farias, C. B., Giacomazzi, J., Alemar, B., Lenz, G., Roesler, R., Schwartsmann, G., Osvaldt, A. B., Hainaut, P., & Ashton-Prolla, P. (2014). PRIMA-1, a mutant p53 reactivator, induces apoptosis and enhances chemotherapeutic cytotoxicity in pancreatic cancer cell lines. *Investigational New Drugs*, *32*(5), 783–794. https://doi.org/10.1007/s10637-014-0090-9

Joerger, A. C., Ang, H. C., & Fersht, A. R. (2006). Structural basis for understanding oncogenic p53 mutations and designing rescue drugs. *Proceedings of the National Academy of Sciences of the United States of America*, *103*(41), 15056–15061. https://doi.org/10.1073/pnas.0607286103

Joerger, A. C., & Fersht, A. R. (2007). Structure-function-rescue: The diverse nature of common p53 cancer mutants. *Oncogene*, *26*(15), 2226–2242. https://doi.org/10.1038/sj.onc.1210291

King, J. C., Lu, Q.-Y., Li, G., Moro, A., Takahashi, H., Chen, M., Go, V. L. W., Reber, H. A., Eibl, G., & Hines, O. J. (2012). Evidence for activation of mutated p53 by apigenin in human pancreatic cancer. *Biochimica et Biophysica Acta*, *1823*(2), 593–604. https://doi.org/10.1016/j.bbamcr.2011.12.008

Kollman, P. A., Massova, I., Reyes, C., Kuhn, B., Huo, S., Chong, L., Lee, M., Lee, T., Duan, Y., Wang, W., Donini, O., Cieplak, P., Srinivasan, J., Case, D. A., & Cheatham, T. E. (2000). Calculating structures and free energies of complex molecules: Combining molecular mechanics and continuum models. *Accounts of Chemical Research*, *33*(12), 889–897. https://doi.org/10.1021/ar000033j

Kopustinskiene, D. M., Jakstas, V., Savickas, A., & Bernatoniene, J. (2020). Flavonoids as anticancer agents. *Nutrients*, *12*(2), 457. https://doi.org/10.3390/nu12020457

Kumari, R., Kumar, R., & Lynn, A., Open Source Drug Discovery Consortium. (2014). g_mmpbsa–a GROMACS tool for high-throughput MM-PBSA calculations. *Journal of Chemical Information and Modeling*, *54*(7), 1951–1962. https://doi.org/10.1021/ci500020m

Liu, X., Wilcken, R., Joerger, A. C., Chuckowree, I. S., Amin, J., Spencer, J., & Fersht, A. R. (2013). Small molecule induced reactivation of mutant p53 in cancer cells. *Nucleic Acids Research*, *41*(12), 6034–6044. https://doi.org/10.1093/nar/gkt305

Londhe, A. M., Gadhe, C. G., Lim, S. M., & Pae, A. N. (2019). Investigation of Molecular Details of Keap1-Nrf2 inhibitors using molecular dynamics and umbrella sampling techniques. *Molecules (Basel, Switzerland)*, *24*(22), 4085. https://doi.org/10.3390/molecules24224085

Malhotra, L., Goyal, H. K. V., Jhuria, S., Dev, K., Kumar, S., Kumar, M., Kaur, P., & Ethayathulla, A. S. (2021). Curcumin rescue p53Y220C in BxPC-3 pancreatic adenocarcinomas cell line: Evidence-based on computational, biophysical, and in vivo studies. *Biochimica et Biophysica Acta. General Subjects*, *1865*(2), 129807. https://doi.org/10.1016/j.bbagen.2020.129807

Malhotra, L., Sharma, S., Hariprasad, G., Dhingra, R., Mishra, V., Sharma, R. S., Kaur, P., & Ethayathulla, A. S. (2022). Mechanism of apoptosis activation by Curcumin rescued mutant p53Y220C in human pancreatic cancer. *Biochimica et Biophysica Acta. Molecular Cell Research*, *1869*(12), 119343. https://doi.org/10.1016/j.bbamcr.2022.119343

Malhotra, L., Singh, A., Kaur, P., & Ethayathulla, A. S. (2023). Comprehensive omics studies of p53 mutants in human cancer. *Briefings in Functional Genomics*, *22*(2), 97–108. https://doi.org/10.1093/bfgp/elac015

Malhotra, L., Singh, A., Kaur, P., & Ethayathulla, A. S. (2023). Phenotypical mapping of TP53 unique missense mutations spectrum in human cancers. https://doi.org/10.1101/2023.02.06.527255

Mark, P., & Nilsson, L. (2001). Structure and dynamics of the TIP3P, SPC, and SPC/E water models at 298 K. *The Journal of Physical Chemistry A*, *105*(43), 9954–9960. https://doi.org/10.1021/jp003020w

Morris, G. M., Huey, R., Lindstrom, W., Sanner, M. F., Belew, R. K., Goodsell, D. S., & Olson, A. J. (2009). AutoDock4 and AutoDockTools4: Automated docking with selective receptor flexibility. *Journal of Computational Chemistry*, *30*(16), 2785–2791. https://doi.org/10.1002/jcc.21256

Motiwale, M., Yadav, N. S., Kumar, S., Kushwaha, T., Choudhir, G., Sharma, S., & Singour, P. K. (2022). Finding potent inhibitors for COVID-19 main protease (Mpro): An in silico approach using SARS-CoV-3CL protease inhibitors for combating CORONA. *Journal of Biomolecular Structure & Dynamics*, *40*(4), 1534–1545. https://doi.org/10.1080/07391102.2020.1829501

Nagao, M., Morita, N., Yahagi, T., Shimizu, M., Kuroyanagi, M., Fukuoka, M., Yoshihira, K., Natori, S., Fujino, T., & Sugimura, T. (1981). Mutagenicities of 61 flavonoids and 11 related compounds. *Environmental Mutagenesis*, *3*(4), 401–419. https://doi.org/10.1002/em.2860030402

Olivier, M., Hollstein, M., & Hainaut, P. (2010). TP53 mutations in human cancers: Origins, consequences, and clinical use. *Cold Spring Harbor Perspectives in Biology*, *2*(1), a001008. https://doi.org/10.1101/cshperspect.a001008

Petersen, H. G. (1995). Accuracy and efficiency of the particle mesh Ewald method. *The Journal of Chemical Physics*, *103*(9), 3668–3679. https://doi.org/10.1063/1.470043

Sang, P., Du, X., Yang, L.-Q., Meng, Z.-H., & Liu, S.-Q. (2017). Molecular motions and free-energy landscape of serine proteinase K in relation to its cold-adaptation: A comparative molecular dynamics simulation study and the underlying mechanisms. *RSC Advances*, *7*(46), 28580–28590. https://doi.org/10.1039/C6RA23230B

Schmid, N., Eichenberger, A. P., Choutko, A., Riniker, S., Winger, M., Mark, A. E., & van Gunsteren, W. F. (2011). Definition and testing of the GROMOS force-field versions 54A7 and 54B7. *European Biophysics Journal: EBJ*, *40*(7), 843–856. https://doi.org/10.1007/s00249-011-0700-9

Schüttelkopf, A. W., & van Aalten, D. M. F. (2004). PRODRG: A tool for high-throughput crystallography of protein-ligand complexes. *Acta Crystallographica. Section D, Biological Crystallography*, *60*(Pt 8), 1355–1363. https://doi.org/10.1107/S0907444904011679

Seeliger, D., & de Groot, B. L. (2010). Ligand docking and binding site analysis with PyMOL and Autodock/Vina. *Journal of Computer-Aided Molecular Design*, *24*(5), 417–422. https://doi.org/10.1007/s10822-010-9352-6

Sharma, S., Malhotra, L., Yadav, P., Mishra, V., Sharma, R. S., & Abdul Samath, E. (2022). Genistein: A novel inhibitor of IL-6/IL-6R interface of the Interleukin-6–mediated STAT3 dependent pathway of carcinogenesis. *Journal of Molecular Structure*, *1258*, 132668. https://doi.org/10.1016/j.molstruc.2022.132668

Srinivasan, J., Cheatham, T. E., Cieplak, P., Kollman, P. A., & Case, D. A. (1998). Continuum solvent studies of the stability of DNA, RNA, and phosphoramidate − DNA helices. *Journal of the American Chemical Society*, *120*(37), 9401–9409. https://doi.org/10.1021/ja981844+

Tavernelli, I., Cotesta, S., & Iorio, E. E. D. (2003). Protein dynamics, thermal stability, and free-energy landscapes: A molecular dynamics investigation. *Biophysical Journal*, *85*(4), 2641–2649. https://doi.org/10.1016/S0006-3495(03)74687-6

Tuli, H. S., Garg, V. K., Bhushan, S., Uttam, V., Sharma, U., Jain, A., Sak, K., Yadav, V., Lorenzo, J. M., Dhama, K., Behl, T., & Sethi, G. (2023). Natural flavonoids exhibit potent anticancer activity by targeting microRNAs in cancer: A signature step hinting towards clinical perfection. *Translational Oncology*, *27*, 101596. https://doi.org/10.1016/j.tranon.2022.101596

van Aalten, D. M. F., Bywater, R., Findlay, J. B. C., Hendlich, M., Hooft, R. W. W., & Vriend, G. (1996). PRODRG, a program for generating molecular topologies and unique molecular descriptors from coordinates of small molecules. *Journal of Computer-Aided Molecular Design*, *10*(3), 255–262. https://doi.org/10.1007/BF00355047

Veeramuthu, D., Raja, W. R. T., Al-Dhabi, N. A., Savarimuthu, I., Veeramuthu, D., Raja, W. R. T., Al-Dhabi, N. A., & Savarimuthu, I. (2017). Flavonoids: Anticancer properties, flavonoids - from biosynthesis to human health. *IntechOpen*, 287. https://doi.org/10.5772/68095

Wales, D. J., & Bogdan, T. V. (2006). Potential energy and free energy landscapes. *The Journal of Physical Chemistry. B*, *110*(42), 20765–20776. https://doi.org/10.1021/jp0680544

Wallace, A. C., Laskowski, R. A., & Thornton, J. M. (1995). LIGPLOT: a program to generate schematic diagrams of protein-ligand interactions. *Protein Engineering*, *8*(2), 127–134. https://doi.org/10.1093/protein/8.2.127

Wang, M., Firrman, J., Liu, L., & Yam, K. (2019). A review on flavonoid apigenin: Dietary intake, ADME, antimicrobial effects, and interactions with human gut microbiota. *BioMed Research International*, *2019*, e7010467. https://doi.org/10.1155/2019/7010467

Yahyavi, M., Falsafi-Zadeh, S., Karimi, Z., Kalatarian, G., & Galehdari, H. (2014). VMD-SS: A graphical user interface plug-in to calculate the protein secondary structure in VMD program. *Bioinformation*, *10*(8), 548–550. https://doi.org/10.6026/97320630010548